Title
Experimental results for hybrid energy storage systems coupled to photovoltaic generation in residential applications

Journal
International Journal of Hydrogen Energy, 36(19)

ISSN
0360-3199

Authors
Maclay, James D
Brouwer, Jacob
Samuelsen, G Scott

Publication Date
2011-09-01

DOI
10.1016/j.ijhydene.2011.06.089

Available at www.sciencedirect.com

ScienceDirect

journal homepage: www.elsevier.com/locate/he

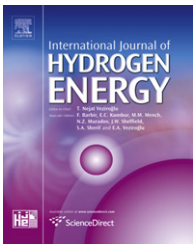

Experimental results for hybrid energy storage systems coupled to photovoltaic generation in residential applications

James D. Maclay, Jacob Brouwer, G. Scott Samuelsen*

National Fuel Cell Research Center, University of California, Irvine, CA 92697-3500, United States

ARTICLE INFO

Article history:
Received 18 October 2010
Received in revised form
2 June 2011
Accepted 17 June 2011
Available online 23 July 2011

Keywords:
Dynamic experimental data
Fuel cell
Electrolyzer
Solar-hydrogen
Hybrid energy storage
Renewable residential power

ABSTRACT

An experimental solar-hydrogen powered residence simulator was built and tested. The system consisted of a solar photovoltaic array connected to an electrolyzer which produced hydrogen as a means of energy storage. The hydrogen was used to produce electricity in a fuel cell that operated in parallel with a battery to meet dynamic power demand similar to that found in residential applications. The study demonstrated the technical feasibility of operating such a system under the simultaneous dynamics of solar input and load. Limitations of current fuel cell and electrolyzer designs, as they pertain to both power delivery and energy storage, were identified. The study also established the need to understand and address dynamic performance in the design and application of solar-hydrogen reversible fuel cell hybrid systems. An economic analysis found that major cost reductions would need to be achieved for such systems to compete with conventional energy storage devices.

1. Introduction

Solar photovoltaic (PV) arrays are increasingly being deployed to meet residential electricity needs. One of the major challenges for PV systems remains matching the sun's diurnal and intermittent power supply with the dynamic and non-coincident power demand of a residence. Operating the PV array in parallel with the electrical grid is one solution to this problem. However, if the PV array is operated independently from the grid, i.e., as a stand-alone power system, some type of energy storage device must be employed. This device must store excess PV energy and subsequently deliver power at the desired time and rate. The energy storage device most commonly used with PV systems today is the rechargeable lead acid battery.

With the emergence of reversible or regenerative fuel cells (RFC), one can consider using a new energy storage device that is both analogous to rechargeable batteries and that may have unique advantages in comparison to them in photovoltaic applications. For example, such systems could produce hydrogen for use as a vehicle fuel or for heating or cooking in addition to energy storage. It is also possible to implement a system design that uses both an RFC and a battery together in a "hybrid" energy storage scenario that combines the strengths of each technology.

Electrolysis is the charge mode of the RFC, where electricity and water are taken in to produce hydrogen and oxygen. The discharge mode uses the fuel cell to take in hydrogen and oxygen (or air) and produce electricity and water. Regenerative fuel cells have a wide range of potential applications including energy storage devices coupled to renewable energy sources, auxiliary power plants for automobiles and aircraft, and propulsion systems for satellites and other space applications.

* *Corresponding author*. Tel.: +1 949 824 1999x221.
E-mail address: jb@nfcrc.uci.edu (J. Brouwer).

0360-3199/$ – see front matter
doi:10.1016/j.ijhydene.2011.06.089

The authors are not aware of prior research that has addressed critical questions that pertain to the use of RFC systems in solar-hydrogen residential applications. These questions are, one, can the electrolyzer be relied upon to consistently produce hydrogen in the presence of dynamic solar input and, two, can the fuel cell be relied upon to deliver power at the dynamic rates typical of residential demand and what are the limitations. This study addresses the technical feasibility of operating a residential solar-hydrogen reversible fuel cell under the conditions of a dynamic source (sun) and sink (load) and establishes the importance of understanding the dynamic requirements of the application and addressing the dynamic performance in design. A cost analysis is also performed to assess the commercial feasibility of such a system.

2. Background and related work

The main groups that are advancing regenerative proton exchange membrane fuel cell systems are at NASA [1], Lawrence Livermore National Laboratory [2], Proton Energy Systems [3], the U.S. Department of Energy [4], and Giner Electrochemical Systems [5]. Other groups that are more focused on bi-functional electrode or MEA development include researchers at AIST in Japan and the Dalian Institute of Chemical Physics in China [6–8]. Few of these research groups have published analyses pertaining to hybrid energy storage systems that contain regenerative fuel cells and batteries as applied to residential solar photovoltaic energy systems as in this effort. However, some recent analyses have addressed related topics.

Kelouwani et al. [9] created a dynamic model consisting of a battery, buck and boost DC converters, electrolyzer, fuel cell and hydrogen storage. Experimentally measured current from a wind generator rectifier and a PV DC regulator were studied as inputs to this energy storage system model. The load on the energy storage system was said to be representative of residential consumption, but the applied residential load and temporal resolution are not described in the paper. The authors claim that the modeled system shows results comparable to the performance of an experimental system with an average deviation of 5%.

Maclay et al. [10] have developed a dynamic empirical model that uses performance curves for an RFC and a battery, measured output from a PV array and measured power demand for an individual residence to determine the optimum sizing of the battery and RFC system for a residence. This study considered the efficiency, load sharing, energy storage capacity and component duty cycle in the dynamic analyses used to determine component sizes. This work was extended [11] to assess control strategies, sizing, capital costs, and efficiencies of RFCs, batteries, and ultra-capacitors both individually, and in combination, as hybrid energy storage devices. The choice of control strategy for a hybrid energy storage system was found to have a significant impact on system efficiency, hydrogen production and component utilization. Uzunoglu et al. [12], Li et al. [13] and Lagorse et al. [14] describe results for similar models with focuses on sizing optimization and control.

Bilodeau and Agbossou [15] build on the work of Kelouwani et al. [9] by using a dynamic fuzzy logic controller to determine suitable hydrogen production and consumption rates based upon system power input and output and the battery state of charge. These rates are then implemented to control the operation of the fuel cell and electrolyzer in the model.

Busquet et al. [16] describe an empirical model of a PEM RFC that can calculate cell voltage vs. current density (VI) curves by entering measured values of stack temperature and oxygen partial pressure.

El-Sharkh et al. [17] have developed a dynamic electrochemical model of a PEM fuel cell and methanol reformer. The main focus of the study was to characterize the transient response and load following capability of the fuel cell under an actual residential load. The results indicate that the fuel cell is able to rapidly respond to residential load changes.

Tanrioven and Alam [18] describe the impact of load management control on the reliability of residential stand-alone fuel cell systems. Reliability evaluation is performed with a component-based state space model that uses fuzzy set theory and expert knowledge. The smart energy management control is said to increase fuel cell reliability from 95% to 99.93% over a ten year operational period.

Gigliucci et al. [19] report results from both the demonstration of a residential fuel cell CHP unit and a mathematical model of the system that predicts technical and economic evaluations of system suitability to specific residential customers.

Santarelli and Macagno [20] developed a thermoeconomic model of a residential solar-hydrogen reversible fuel cell system. They find that the system has a very high cost but suggest that it may be a viable solution for remote stand-alone applications without electrical distribution infrastructure. The analysis uses average hourly load and solar irradiance data, which will not capture the actual power demand rates that the fuel cell will have to meet or the true solar dynamics that the electrolyzer will be subject to.

Yilanci et al. [21] provide energy and exergy analyses for a model based on a 1.2 kWe Nexa PEM fuel cell unit in a solar-based hydrogen production system. A parametric study on the system and its parameters was undertaken to investigate the changes in the efficiencies for variations in temperature, pressure and anode stoichiometry. Energy and exergy efficiencies were found to increase with pressure, not change with increasing temperature and decrease with increasing anode stoichiometry. The results show that the PEM fuel-cell system has lower exergy efficiencies than the corresponding energy efficiencies due to irreversibilities not considered by energy analysis.

Guizzi et al. [22] describe experimental results for a hybrid energy system for electric wheelchair and industrial automated guided vehicle applications. The main components are a PEM fuel cell, a battery pack and an ultra-capacitor pack as power sources, and metal hydride canisters as energy storage devices. Overall system efficiency is reported to be always higher than 36%. The fuel cell meets low to medium loads, which allows near maximum efficiency operation.

Douceta et al. [23] report the general performance for an auxiliary power unit consisting of a PEM water electrolyzer, a hydride storage tank and a fuel cell. The hydrogen can be

used for co-generation of heat and electricity in residential, remote site or mobile hydrogen refueling applications. There is no mention of how the system may respond to actual residential loads.

Eroglu et al. [24] describe results for an experimental system that uses solar and wind energy and a reversible fuel cell and battery for energy storage. However, there is no mention of the impact of dynamic solar irradiance or load demand on system performance.

3. Approach

The current study analyzes an experimental hybrid energy storage system consisting of an electrolyzer, fuel cell and battery coupled to a solar photovoltaic system, intended for use in residential applications. A schematic of the experimental system and all of its components is shown in Fig. 1.

The nine main components of the experimental residential power system are a PV array (Unisolar, 5 kW (PTC) amorphous silicon), utility grid (Southern California Edison), electrolyzer (Proton Energy Systems, Hogen RE-40), hydrogen storage tank, fuel cell (ReliOn, Independence 1000), inverter (ExelTech, XP 1100), load bank and data acquisition.

The PV was wired directly to the electrolyzer. The electrolyzer design allows for a DC voltage input range of 60–200 VDC and maximum current and power limits of 150 ADC and 10 kW, respectively. Three electrolyzer operational modes are available 1) grid power only, 2) PV power only, and 3) a PV/grid mixture that preferentially uses PV power. Hydrogen from the electrolyzer is delivered at 1380 kPa at a purity of >99.999% with <5 ppm H_2O and <1 ppm of other gases. The nominal maximum hydrogen production rate is 1 Nm^3/hr. The electrolyzer uses a maximum of 21 L of water per day and requires deionized water at >1.0 MΩ cm. A mass flow meter (Sierra Instruments: Model Flo-Box 840M-4-OV1-SK1-D-V1-S1-MP) was used to measure hydrogen flow rate from the electrolyzer.

The tank used to store hydrogen generated by the electrolyzer was an Air Gas Type 200 compressed gas cylinder, with an internal volume of 0.04 m^3. If hydrogen is stored at 1380 kPa then it should contain 1.95 kWh of energy (HHV). This tank was used intermittently throughout testing and acted as an accumulator between the electrolyzer and fuel cell.

The ReliOn PEM fuel cell is rated to deliver 1000 W of power at 48 VDC and 20 ADC. It requires a minimum of 99.95% pure hydrogen at 28–41 kPa supply pressure. Approximate hydrogen fuel consumption is 15 SLPM at 1000 W and 6.5 SLPM at 500 W. The fuel cell operating temperature range is 0–45 °C. The unit also comes with a battery bank that is operated in parallel with the fuel cell stack to provide power to the load. This battery cannot be disconnected without shutting down the system and so the fuel cell cannot operate independently from the battery. The fuel cell can be operated in two modes 1) as a power source and 2) as a battery charger. The power source mode was employed during all the current experiments. A power analyzer (Yokogawa: Model WT 1600) was used to characterize fuel cell system, fuel cell stack and battery performance.

The fuel cell system DC power output was connected to a true sine wave inverter rated for 41.5–62 VDC input and an output of 1100 WAC at 120 VAC. The inverter will shut down if the input voltage requirements are not met. The Yokogawa

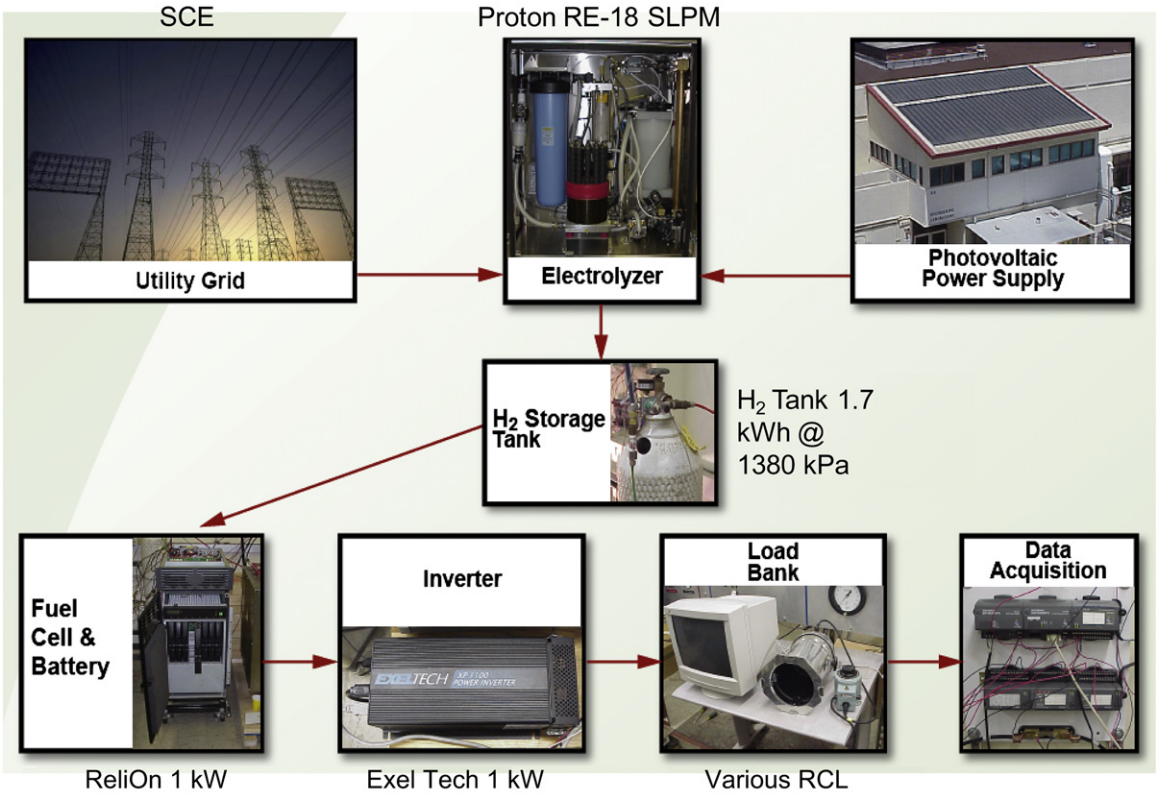

Fig. 1 – Set-up of experimental renewable reversible fuel cell system.

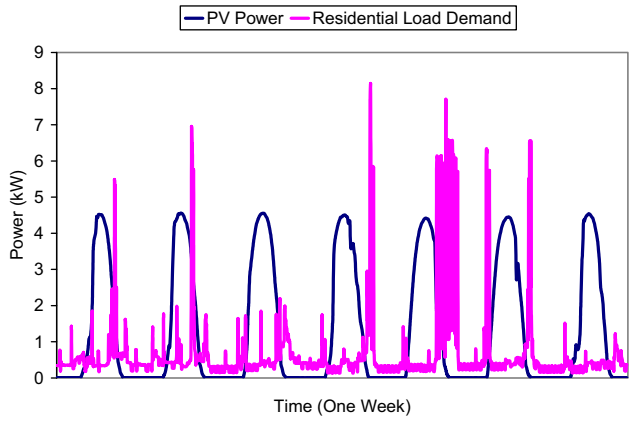

Fig. 2 – Weekly electrical load demand for a six-person family home in Irvine, California and photovoltaic electrical power supply from a 5 kW array.

power analyzer was used to measure inverter current and voltage outputs.

An AC load bank was constructed in order to test dynamic loads similar to those measured in residences. The load bank consisted of resistive, inductive and capacitive loads connected to the inverter. Resistive loads included a bank of lights with three 100 W, one 85 W and one 25 W incandescent light bulbs. A 1000 W incandescent light source was connected to a variable auto-transformer (which is itself an inductive load) in order to smoothly sweep power from 0 to 1000 W. Inductive loads included a 300 W variable speed blender and a 746 W vacuum pump. Capacitive loads included a 264 W television and four cathode ray tube (CRT) computer monitors rated at 240 W each. All load components where manually operated.

Data were collected at 2 s discrete and 1 min average intervals using LabVIEW 7.0 software made by National Instruments. Field Point modules made by National Instruments were used as the interface between analog input sensor signals sent from the test bed and the digital output signals sent to LabVIEW.

As the Background section suggests, attention and interest in the application of fuel cells for residential and other small and highly dynamic end uses has recently increased. The work contained herein expands upon current understanding and is novel in that it addresses the experimental ability of the electrolyzer to produce hydrogen when powered by dynamic solar input and the experimental ability of the fuel cell to meet dynamic residential load demand.

4. Dynamic data

The dynamic data for PV power output (kW vs. time (s)) were determined by measurement of a Unisolar 5 kW (PTC) amorphous PV array installed at the University of California, Irvine (Latitude: 33.6 N, Longitude: 117.7 W). LabVIEW data acquisition software was used to collect power output data on a time interval of every 2 s. One week of data was acquired from 8/2/01–8/9/01; the only PV data not measured at 2 s resolution are presented in Fig. 2 and were collected on a 15 min interval.

The dynamic data for residential power demand (kW vs. time (s)) were collected from a 6-person family home in Irvine California (Latitude: 33.6 N, Longitude: 117.7 W) using a Dent Instruments (Elite Pro Model) meter and logged at 3 s integrated time intervals. A week of data, acquired from 8/2/03–8/9/03, comprised the primary data set for the analyses presented herein. The major electrical devices used within the residence included an electric oven, washer and dryer, refrigerator, coffee maker, microwave, hair dryer, television, computers and lighting. The oven was determined to account for some of the largest peaks and power dynamics observed during evening hours. Air conditioning, which is common to many of the residences throughout the Western U.S., was not present in this particular residence.

5. Results & discussion

5.1. *Measured dynamic residential power demand and PV power output*

The measured electrical power demand of the residence and the measured electrical power production of the PV array spanning the same week of 8/2/03–8/9/03 are presented in Fig. 2. The total electrical energy required by the home was 108.1 kWh (15.4 kWh/day on average) and the total energy supplied by the PV array was 224.8 kWh (32.1 kWh/day on average). It is clear from Fig. 2 that most of the power demand for the residence occurs in the morning and evening when there is low solar availability. It is also clear that most of the PV power output goes unused during midday. This time offset between supply and demand leads to only 33.6% (36.3 kWh) of the residential power demand possibly being met directly by the PV, with 66.4% (71.8 kWh) of the demand requiring grid power or some type of energy storage device.

Fig. 3 shows residential power demand ramp rate data collected at a 3 s sampling rate, over a single day. The maximum power demand ramp was 1895 W/s and the maximum load shed was −1827 W/s. The 3 s data were compared to data collected simultaneously on the same circuits at a 5 min sampling rate (data not shown). The maximum power demand ramp for the 5 min data set was 21.6 W/s and the maximum load shed was −18.1 W/s. This

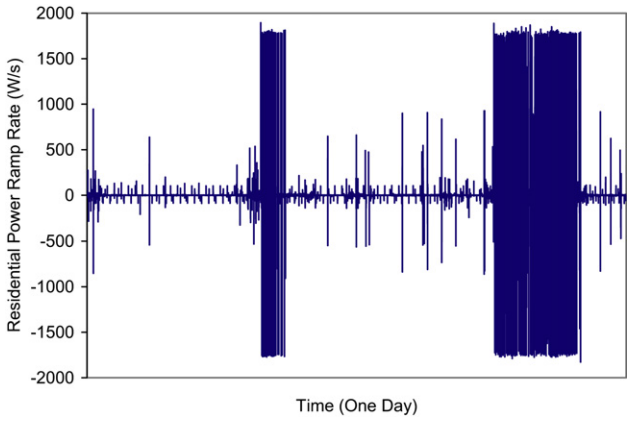

Fig. 3 – Daily residential demand power ramp rates.

dramatic difference between ramp rates underscores the need for high resolution data sets for accurate characterization of real load demands that will be experienced by stand alone power systems.

For the experimental solar-hydrogen residential system results, (Fig. 4–10), the data sampling rate (either 2 s discrete or 1 min averaged) and electrolyzer mode (either PV-only or grid-only mode) are indicated. Fig. 4 shows PV DC power input to the electrolyzer, the equivalent power output of the hydrogen evolved from the electrolyzer and the cumulative raw hydrogen energy produced over the span of a day. PV energy consumption by the electrolyzer was 33.4 kWh/day, grid energy consumption was 4.8 kWh/day and hydrogen energy production was 17.8 kWh/day. Grid AC power consumption, which is required by the electrolyzer to run ancillary components such as an air blower and water pump even in PV-only mode, was 430 W on average. Cumulative hydrogen energy production of 17.8 kWh/day is greater than the 15.4 kWh/day average residential load demand. However, if this hydrogen was to be used in a fuel cell to power the residence it would be insufficient to meet the total energy requirements due to losses in the fuel cell.

The electrolyzer was able to successfully operate with 518 W of PV power upon start up at 7:07 AM as shown in Fig. 4. Prior to this, the electrolyzer failed to start due to low cell voltage and low system pressure errors. The internal pressure must build to 1380 kPa before the electrolyzer can deliver hydrogen and PV power below 518 W was insufficient to achieve this internal pressure requirement. The electrolyzer shut down at 6:26 PM with a PV power input of 212 W due to a low system pressure error. The electrolyzer stack operated continuously throughout the day for 11 h and 19 min in the PV-only mode since solar irradiance was fairly uninterrupted by clouds. In general, the electrolyzer tolerated short transients in solar irradiance, such as intermittent cloud cover. Extended transients in solar irradiance, such as cloudy days with rain, led to electrolyzer shut downs due to system pressure loss. Thus, the electrolyzer was found to be able to consistently produce hydrogen in the presence of dynamic solar irradiance as long as system pressure can be maintained.

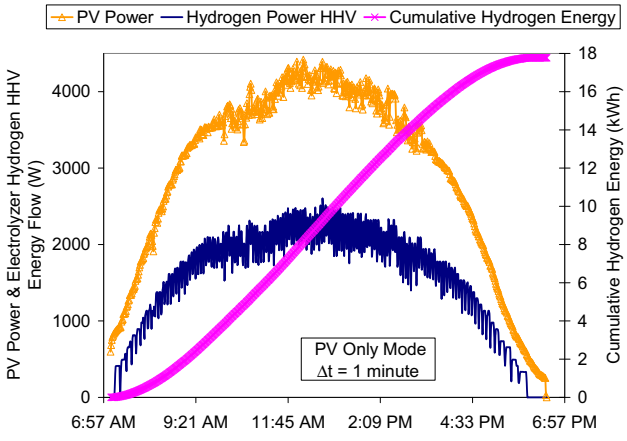

Fig. 4 – Daily PV power output, electrolyzer hydrogen energy flow and cumulative daily hydrogen energy produced.

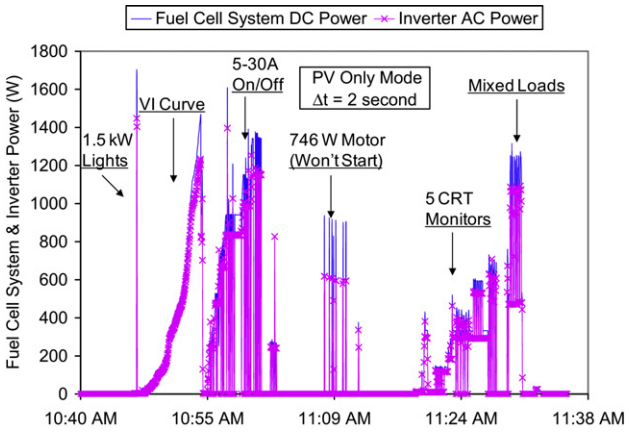

Fig. 5 – Independence 1000 fuel cell system DC power and inverter AC power outputs during dynamic load testing.

Now that hydrogen has been produced by the electrolyzer and stored in a gas cylinder, it can be used in the fuel cell to meet a simulated residential load dynamics. A key interest of this research is to determine the ability of a fuel cell to meet the fast power rates of change observed in residential demand profiles (Fig. 3). Although the experimental fuel cell and inverter are only sized to a maximum continuous rated power output of 1 kW (versus the peak demand of over 8 kW seen in the residence in Fig. 2), it will be useful to see if the power ramp rates measured in Fig. 3 can be approached by the system. Another interest is to determine whether the experimental system has the ability to supply reactive loads with low power factors where inductive and capacitive power demands are significant.

Fig. 5 shows fuel cell system DC power output, which is a measure of the total combined output of the fuel cell stack and internal battery to the load. Inverter AC power output is also shown in Fig. 5, which is in response to the actual power demand of the AC load bank. For this set of experiments (Figs. 5 and 6), the fuel cell power output was only being measured at the system level and so it was not possible to determine

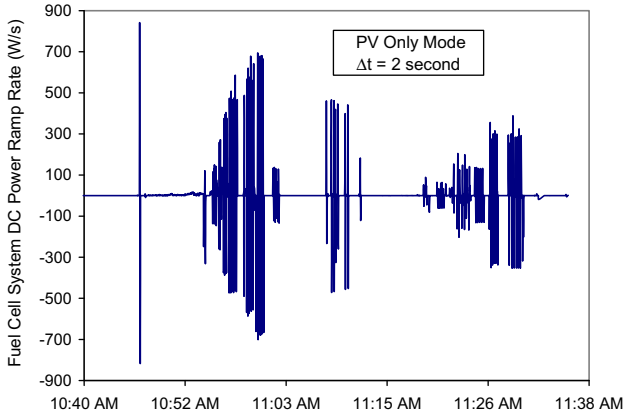

Fig. 6 – Independence 1000 fuel cell system DC power ramp rates during dynamic load testing.

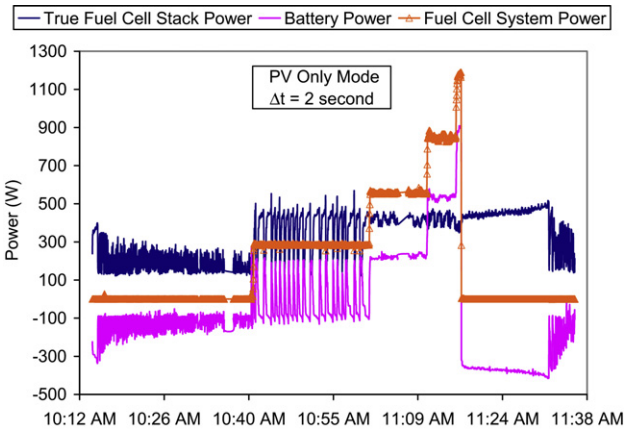

Fig. 7 – Independence 1000 fuel cell system, stack and battery power.

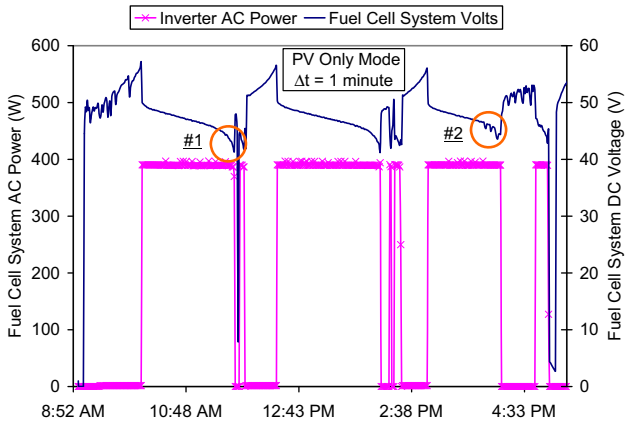

Fig. 9 – Independence 1000 fuel cell system voltage and AC power demand.

what portion of the load was being met by the fuel cell stack and what portion was being met by the battery.

The simulated experimental residential loads applied in Fig. 5 will be described in progression, moving from left to right in the figure. The first load applied was resistive, where approximately 1400 W of incandescent lights were switched on and off simultaneously. This event corresponded to the fastest observable ramp rates of 842 W/s and −817 W/s. The fuel cell system was able to meet this dynamic load demand without a problem.

Power was then slowly increased using a variable transformer to power increasing amounts of incandescent light to create a VI curve. It was observed that as power demand from the fuel cell system increases the amount of DC power needed to produce a given amount of AC power increases. This is a function of inverter efficiency which decreases above an output power of 1000 W.

Next, between 5 and 30 A of DC current was switched on and off five times for each of the 5 A increments (i.e., 5, 10, 15, 20, 25 and 30 A) using a resistive AC load bank. The fuel cell system was able to meet this set of load demands without exception.

Next, two inductive loads were applied to the fuel cell system at separate times. The first load is a variable speed blender that draws approximately 250 W of power. Power to the blender was cycled five times without a problem. One of the blender motor starts produced a momentary power spike of 830 W. The second inductive load test utilized a vacuum pump rated at 746 W. Eight attempts were made to start the vacuum pump without success. During these attempts inverter voltage dropped from its rated output of 120 V–40 V causing the inverter to shutdown. Fuel cell system voltage drops to 50 V during this motor start event, which is within the inverter operational input range of 41.5–62 VDC. The fuel cell system itself did not shut down during these motor start events because it is a DC source and does not have to produce reactive power, whereas the inverter, an AC source, does. The vacuum pump was plugged into a 120 VAC wall socket and probed using a clamp-on ammeter during multiple successful start up events. The resulting inrush current ranged from 28 to 39 A, which translates to 3360–4680 W. The inverter proved unable to function under the strain of the inrush current associated with the vacuum pump motor start. This was the only instance of a system shutdown during the dynamic load

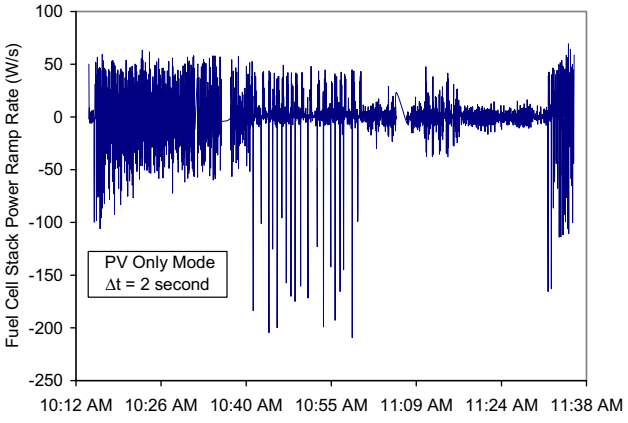

Fig. 8 – Independence 1000 fuel cell stack power ramp rates.

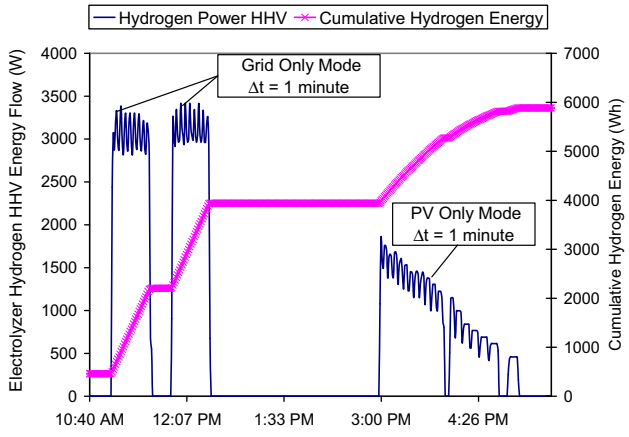

Fig. 10 – Electrolyzer hydrogen energy flow and cumulative hydrogen energy.

testing. The lowest power factor measured during the inductive load tests was 0.79.

Next, dynamic capacitive load testing was carried out. First, a television was turned on together with some incandescent lights and then the television was cycled six times by itself. Second, the television along with 4 cathode ray tube (CRT) computer monitors were cycled on and off six times. The fuel cell system was able to power these dynamic events without a problem. A peak in demand of 100 W above the steady state demand is observed in association with the start up of the five CRTs. The television by itself is capable of drawing the power factor down to 0.18 upon start up and has a resting capacitance that leads to a power factor of 0.3 even when not powered. When plugged in but not in use, the television still draws 10 W of power due to slow charging of the capacitive CRT. The CRT monitors have less capacitive reactance than the television and during combined operation a power factor of 0.65 was observed.

Finally, mixed loads were cycled. First, the blender was left on and the five CRTs were cycled, leading to an improved power factor of 0.77 vs. 0.65 for the case of CRT use only (more capacitive loads). Next, the blender was cycled with the five CRTs. Finally, 485 W of incandescent lights were left on and the blender and five CRTs were cycled together leading to a power factor of 0.93. Again, the fuel cell system was able to power these dynamic loads without a problem.

Fig. 6 shows the power ramp rates experienced by the fuel cell system when subjected to the load tests of Fig. 5. The maximum power ramp rate measured was 842 W/s and the maximum load shed measured was −817 W/s. These values are less than half those measured for the residence in Fig. 3, but the system is able to output close to its maximum power rating of 1000 W within 1 s. A larger power class fuel cell system would likely be able to meet the power rates observed in the residence. Throughout the dynamic load testing there was only one instance of a system shutdown and this was caused by an inverter failure. The system was able to follow the load dynamics in all other instances.

The results presented thus far characterize fuel cell system power, which is a combination of fuel cell stack and battery power. Fig. 7 presents results from investigating the dynamic response of the fuel cell system, fuel cell stack and battery power as successive loads were applied to the fuel cell system in stepwise fashion. In the region before 10:40 AM, when no external power is consumed, the fuel cell stack is float charging the battery. When an external AC load of 250 W is added to the fuel cell, the fuel cell alternates between powering the load and charging the battery while the battery correspondingly alternates between charging and discharging. Once the external load reaches 500 W, the fuel cell and battery both contribute continuous power to the load (no charging of the battery occurs). As the load is stepped up to 750 W and then 1000 W, the fuel cell remains at a continuous output of approximately 450 W while the battery steps up its power output to meet the increased load demand. When the external load is removed, the fuel cell stack begins charging the battery first by bulk charging and eventually by float charging.

Fig. 8 shows fuel cell stack power rates of change for the case shown in Fig. 7. Power ramp rates up to 67 W/s and load sheds up to −209 W/s were measured. These are insufficient to meet the ramp rates seen for the residence (Fig. 3). The fastest power rates of change occur during battery charging.

The design of this fuel cell system uses the fuel cell as a base-load power device and the battery as a peak-load power device. This is a wise design strategy since the fuel cell has greater physical limitations (such as control and delivery of fuel and oxidant) compared to the battery. However, these results do not help determine whether fuel cells, when not hybridized with batteries and designed to operate in this fashion, can meet the fast power demand ramp rates observed in residences.

The next line of inquiry was to characterize the energy storage capacity of the fuel cell system, without a hydrogen tank to store energy. This was done by subjecting the system to a constant 400 W AC load consisting of incandescent lights, on a relatively sunny day with the system operating in PV-only mode.

Fuel cell system AC power and DC voltage over the span of the experiment are shown in Fig. 9. The voltage initially rises as the internal battery is charged, then the load is applied and the voltage drops significantly; finally voltage falls precipitously in the case of system shutdowns (circle #1 in Fig. 9). This voltage profile is repeated roughly three times during the test (Fig. 9). Six out of the seven failures observed during this testing were due to the fuel cell system reaching the low voltage input limit of the inverter. This voltage decay occurs because the fuel cell cannot meet the 400 W load demand by itself and so it relies on the internal battery for assistance. The battery is unable to maintain a steady voltage for long periods due to its low energy storage capacity. The inverter has a cut out voltage limit of 41.5 V for a nominal 48 V system for a reason. 12 V batteries are deemed to be fully discharged when they reach 10.5 V under discharge. For a 48 V nominal system this is 42 V, so the inverter protects the battery from damage that would otherwise occur in the case that it is discharged below this voltage.

The one failure not caused by low fuel cell system voltage was due to low electrolyzer system pressure, which occurs at 4:57 PM. This loss in system pressure is the result of insufficient solar irradiance. The product pressure drops below the minimum 35 kPa required by the fuel cell to operate at 3:53 PM. As a result, the fuel cell voltage drop oscillates unlike the smooth continuous drop observed when sufficient hydrogen is present (circle #2 in Fig. 9). This voltage oscillation also occurs when the fuel cell is charging the battery in the presence of insufficient hydrogen (at approximately 4:30 PM).

Fig. 10 reveals the difference in hydrogen energy flow from the electrolyzer in grid-only mode during midday and in PV-only mode late in the day. The cumulative energy stored in the hydrogen tank from the two tank fills during midday (area under each hydrogen power curve shown for the grid-only mode case) were measured at 1742 Wh for the first fill and 1739 Wh for the second fill. This is 11% less than the 1950 Wh calculated as the maximum hydrogen storage possible for the tank. Assuming an average residential load of 15.4 kWh and a fuel cell of 40% efficiency, one can determine that 22.3 of these storage tanks would be needed for the fuel cell to meet the day's energy needs (without the battery) if hydrogen were

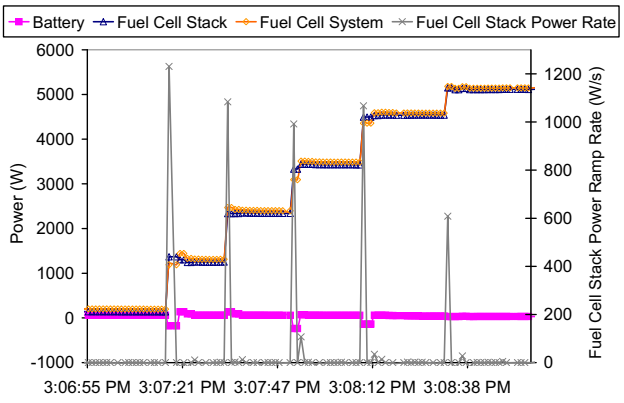

Fig. 11 – GenCore fuel cell system, stack and battery power and fuel cell stack power ramp rates during power loading.

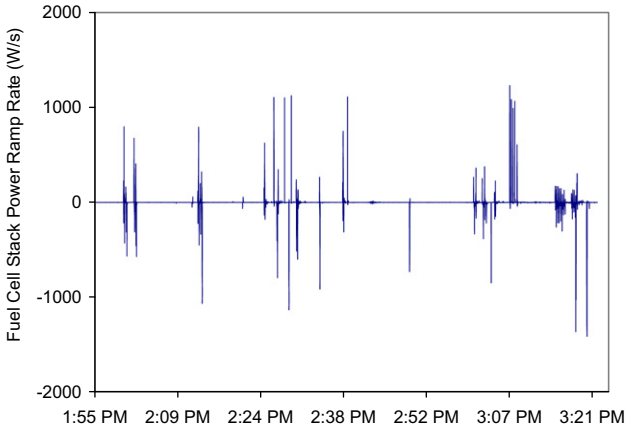

Fig. 13 – GenCore fuel cell stack power ramp rates.

stored at 1380 kPa (at 1.74 kWh per tank). Higher pressure hydrogen storage would most likely be preferable.

In an effort to understand more generally the ability of a PEM fuel cell stack to meet dynamic load ramp rates, data from a Plug Power, 5 kW GenCore system tested at the NFCRC, was analyzed. This fuel cell is marketed for telecommunication back-up power applications, but could be adapted for residential power or other uses. The GenCore is designed for operation on 99.95% pure hydrogen, provides a 48 VDC output and the fuel cell stack operates in parallel with a 48 VDC battery bank.

Fig. 11 shows the GenCore fuel cell system, stack and battery power and fuel cell stack power ramp rates during power loading. The external load, which is a variable resistive load bank, was incrementally increased to the fuel cell system. The power ramp rates for the stack are shown as increasing with these step changes in power. Power ramp rates up to 1231 W/s can be observed for the fuel cell stack alone in Fig. 11.

Fig. 12 shows power ramp rates for the GenCore fuel cell system (with both fuel cell and battery power production). The maximum demand power ramp rate was 1720 W/s, which is 34% of the rated 5 kW GenCore output per second. The maximum load shed power ramp rate was −4352 W/s, which is 87% of the rated 5 kW GenCore output per second. These values represent the response time of the fuel cell system indicating that the hybrid system with the battery allows both faster increasing and decreasing (shed) power ramp rates than the fuel cell stack by itself. These ramp rates come close to or exceed the maximum power ramp rates observed for the residence during 3 s resolution demand monitoring. The maximum fuel cell system power ramp rate of 1720 W/s is 91% of the 1895 W/s observed in the residence and the maximum fuel cell load shed ramp rate of −4352 W/s is 238% of the −1827 W/s observed in the residence.

Fig. 13 shows power ramp rates for the GenCore fuel cell stack. The maximum demand power ramp rate was 1231 W/s, which is 25% of the rated 5 kW GenCore output per second. The maximum load shed power ramp rate was −1412 W/s, which is 28% of the rated 5 kW GenCore output per second. The maximum fuel cell power ramp rate of 1231 W/s is 65% of the 1895 W/s observed in the home and the maximum fuel cell load shed ramp rate of −1412 W/s is 77% of the −1827 W/s observed in the home. These data indicate that unlike the Independence 1000 design, the GenCore hybrid fuel cell with battery design allows the fuel cell stack to load follow and the battery to absorb fuel cell power overshoots (observed in Fig. 11).

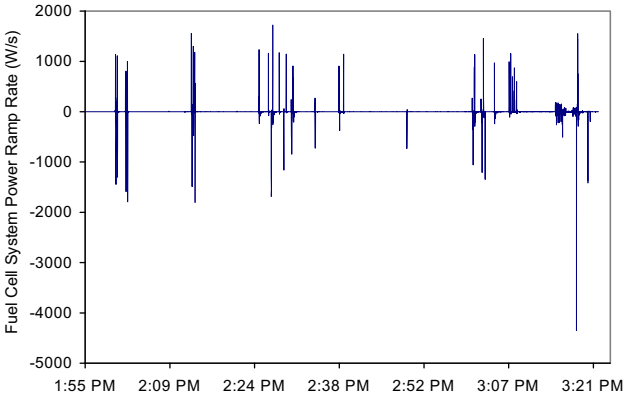

Fig. 12 – GenCore fuel cell system power ramp rates.

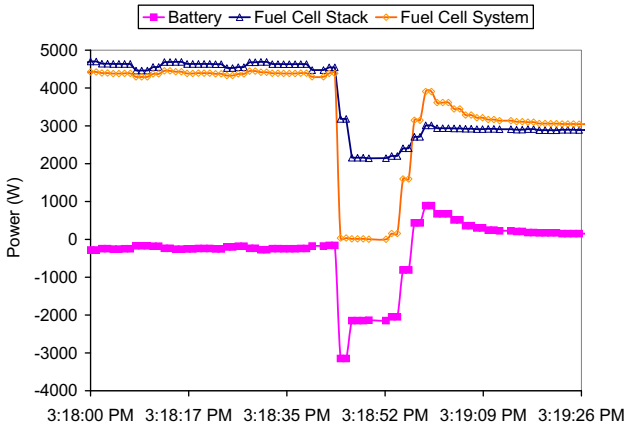

Fig. 14 – GenCore fuel cell system, stack and battery power during dynamic load following.

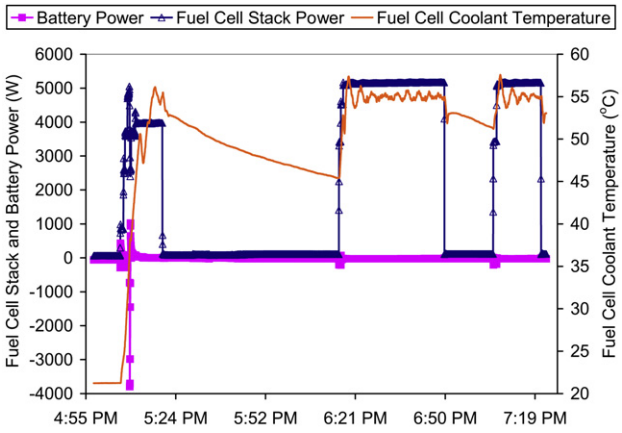

Fig. 15 – GenCore fuel cell stack and battery power and fuel cell coolant temperature (macro view).

Fig. 14 shows the case when load on the fuel cell system is dropped from approximately 4.5 kW–0 kW. The battery can be seen acting as a sink for fuel cell stack power in this event. The fuel cell stack remains in a standby power mode (charging the battery when there is zero load) and then reverts to meeting load demand, once it returns to a nonzero value, approximately 15 s later.

Fig. 15 shows fuel cell stack and battery power and fuel cell coolant temperature for the GenCore. In this test, load demand up to at least 4000 W was added on three separate occasions with fuel cell stack coolant temperature generally increasing with progressive additions of load.

Fig. 16 provides a close-up view of the data presented in Fig. 15, where battery power can be resolved. It is evident that as the fuel cell stack temperature increases, less assistance from the battery is required to meet the load. This indicates that fuel cell stack power ramp rates may be kinetically limited since the increased temperature led to increased dynamic response capability. This is likely due to the fact that increasing operating temperature increases the catalytic activity of the electrodes. Thus, higher power ramp rates should be possible with higher temperature PEM fuel cells.

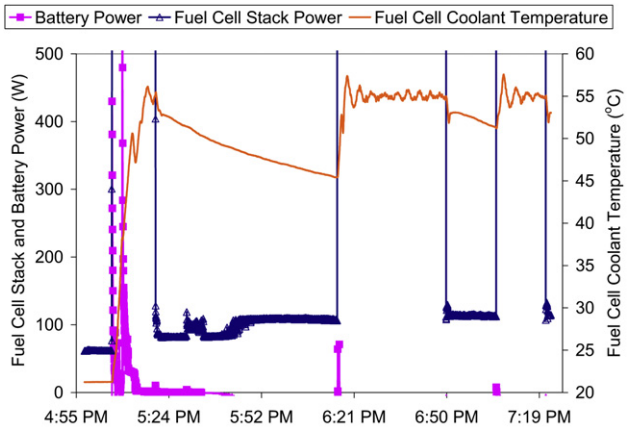

Fig. 16 – GenCore fuel cell stack and battery power and fuel cell coolant temperature (magnified view).

The GenCore uses a heater powered by the battery to heat the fuel cell stack in cases when stack temperature is too low.

5.2. *Solar hydrogen economics*

The majority of this study has focused on the technical feasibility of solar hydrogen and reversible fuel cells for residential applications. This section addresses another significant challenge for the use of these systems today, which is their economic value proposition. Table 1 summarizes all the assumptions and conversions factors that went into the economic analysis.

All analyses assume the HHV of hydrogen. Component capital costs, lifetimes, efficiencies and hydrogen production rates refer to the systems used in this study. The commercial cost of the reversible fuel cell used during experimentation is $10,500/kW, which agrees well with the value of $10,000/kW used in the model.

Table 2 shows the results of the economic analysis, which is based upon the measured performance and cost of current components (not state-of-the-art). Note that accounting for a dynamic load profile, as opposed to a steady state analysis at a design point, reduces the economic performance of the system.

The cost of electricity from PV (generation not retail) is 124% of the California average retail electricity price. The cost of raw solar-hydrogen energy using PV-electrolysis is 106% of grid-electrolysis generated hydrogen. Electricity derived from

Table 1 – Solar hydrogen economic analysis assumptions and conversions.

		Units
Hydrogen HHV	39.7	kWh/kg
Hydrogen Mass/Volume Conversion	11.11	Nm^3/kg
Electrolyzer Capital Cost	75,000	$/Unit
Electrolyzer Capital Cost	7500	$/kW Input
Electrolyzer Maximum Hydrogen Production Rate	1.16	Nm^3/hr
Electrolyzer Efficiency	41.5	%
Capital Cost per Battery	191	$
Battery Voltage	6	V
Battery Amp-Hour Rating (C/20)	350	Ahr
Battery Discharge Time	20	hr
Battery Depth of Discharge	50	%
Battery Cycle Lifetime (for 50% Depth of Discharge)	1000	Cycles
Battery Cycle per Day	1	Cycle/day
Battery Percent of Time Discharging	40	% Time
Battery Percent of Time Charging	60	% Time
Battery Efficiency During Charge	90	%
Average Battery Efficiency During Charge/Discharge	94	%
Battery Capital Cost (C/20 Rate) 100% Raw Energy Rating	91	$/kWh
Fuel Cell Capital Cost	3000	$/Unit
Fuel Cell Capital Cost	3000	$/kW Output
Fuel Cell Efficiency	40	%
PV Lifetime (Continuous Operation)	30	Yr
Electrolyzer Lifetime (Continuous Operation)	6	Yr
Battery Lifetime (Continuous Operation)	2.75	Yr
Fuel Cell Lifetime (Continuous Operation)	2.28	Yr

Table 2 – Economic analysis of energy costs.

	Energy Cost ($/kWh)	HHV Energy Cost ($/kg*$H_2$)
Assumed Average California Retail Electricity Price	0.125	NA
Assumed Photovoltaic Electrical Generation Cost	0.155	NA
Battery Electrical Generation Capital Cost	0.402	NA
Electrolyzer Hydrogen Generation Capital Cost (Raw Thermal Hydrogen Energy)	0.344	13.67
Electrolyzer Hydrogen Generation Capital Cost (Electrical w/40% Efficient Fuel Cell)	0.861	NA
PV + Rechargeable Battery Electrical Generation Capital Cost	0.557	NA
PV + Electrolyzer Hydrogen Capital Cost (Raw Thermal Hydrogen Energy)	0.499	19.82
PV + Electrolyzer Hydrogen Capital Cost (Electrical w/40% Efficient Fuel Cell)	1.016	NA
Fuel Cell Electrical Generation Capital Cost	0.150	NA
PV + RFC Electrical Generation Capital Cost	1.166	NA
California Grid + Electrolyzer Hydrogen Generation Capital Cost	0.469	18.63
California Grid + RFC Electrical Generation Capital Cost	0.986	NA

a reversible fuel cell costs $1.166/kWh or 933% of the California average retail electricity price. Electricity derived from a rechargeable battery costs $0.577/kWh or 462% of the California average retail electricity price.

Compared to PV-battery electricity at $0.577/kWh, PV-RFC electricity is $1.166/kWh or 202% more costly. Electrolyzer capital cost leads to the highest cost per unit energy along the chain of energy costs. These economic analyses suggest that both electrolyzer and fuel cell costs must come down significantly and lifetimes must increase for reversible fuel cells to become cost competitive with conventional energy storage.

The key contribution of the current economic analysis is to establish the baseline cost of current technologies that are required to meet real dynamic residential loads.

6. Summary & conclusions

An experimental solar-hydrogen reversible fuel cell system was tested to determine its viability for residential applications. Most importantly, the current work demonstrates the technical feasibility of the system to operate reliably under dynamic solar irradiance and dynamic loads. It also establishes the importance of considering the real dynamics of the sources and sinks in the design and application of such systems. An economic analysis of the system showed that it is far from being cost competitive.

The electrolyzer (a Proton Energy Systems, Hogen RE-40) was able to consistently produce hydrogen in the presence of dynamic solar irradiance as long as system pressure was maintained.

Two separate fuel cell systems (a 1 kW ReliOn, Independence 1000 and a 5 kW Plug Power, GenCore) were found to possess power ramp rate capabilities of 0.8 and 1.7 kW/s, respectively, compared to the 1.9 kW/s power ramp rate demand measured in the residence. Fuel cell system load shed capabilities were −0.8 and −4.4 kW/s, for the Independence 1000 and GenCore systems, respectively, compared to the −1.8 kW/s power ramp rate measured in the residence. The fuel cell stacks tested were integrated in hybrid systems that produced power in parallel with batteries. The hybrid system integration of batteries with a fuel cell stack is an effective strategy for meeting fast power ramps and load sheds. This configuration also allows the fuel cell to maintain operating temperature (and good electrochemical kinetics) by allowing it to charge the battery when load is reduced. Load following capability of the fuel cell stack alone was observed to increase with fuel cell stack operating temperature.

For stand-alone solar energy storage, the capital cost of the reversible fuel cell was found to be 202% more than a battery. This suggests that both electrolyzer and fuel cell costs must come down significantly for reversible fuel cells to become cost competitive with conventional energy storage.

Acknowledgments

We gratefully acknowledge the support of the U.S. Department of Defense Fuel Cell Program of the Engineer Research and Development Center at the Construction Engineering Research Laboratory, which sponsored this research. We especially acknowledge the support and guidance of the program manager Mr. Frank Holcomb.

REFERENCES

[1] Burke KA. First international energy conversion engineering conference; 2003. August17–21.
[2] Mitlitsky F, Myers B, Weisberg AH. Energy & Fuels. 1998;12:56–71.
[3] Smith W. J Power Sources 2000;86:74–83.
[4] Milliken CE, Ruhl RC. Proceeding of the 2002 U.S. DOE Hydrogen Program Review, (2002).
[5] Giner Electrochemical Systems. LLC delivers a lightweight, 15-kilowatt electrolyzer stack for the Helios prototype flying wing, www.ginerinc.com/lightwei.htm; 2001.
[6] Chaurasia PBL, Ando Y, Tanaka T. Energy Conversion Manage 2003;44:611–28.
[7] Zhigang S, Baolian Y, Ming H. J Power Sources 1999;79:82–5.
[8] Ioroi T, Oku T, Yasuda K, Kumagai N, Miyazaki Y. J Power Sources 2003;124:385–9.
[9] Kelouwani S, Agbossou K, Chahine R. J Power Sources 2005;140:392–9.
[10] Maclay JD, Brouwer J, Samuelsen GS. Intl J Hydrogen Energy 2006;31:994–1009.
[11] Maclay JD, Brouwer J, Samuelsen GS. J. Power Sources 2007;163:916–25.

[12] Uzunoglu M, Onar OC, Alam MS. Renewable Energy 2009;34:509–20.
[13] Li CH, Zhu XJ, Cao GY, Sui S, Hu MR. Renewable Energy 2009;34:815–26.
[14] Lagorse J, Paire D, Miraoui A. Renewable Energy 2009;34:683–91.
[15] Bilodeau A, Agbossou K. J Power Sources 2006;162:757–64.
[16] Busquet S, Hubert CE, Labbe J, Mayer D, Metkemeijer R. J Power Sources 2004;134:41–8.
[17] El-Sharkh MY, Rahman A, Alam MS, Byrne PC, Sakla AA, Thomas T. J Power Sources 2004;138:199–204.
[18] Tanrioven M, Alam MS. J Power Sources 2005;142:264–78.
[19] Gigliucci G, Petruzzi L, Cerelli E, Garzisi A, La Mendola A. J Power Sources 2004;131:62–8.
[20] Santarelli M, Macagno S. Energy Conversion Manage 2004;45:427–51.
[21] Yilanci A, Dincer I, Ozturk HK. Intl J Hydrogen Energy 2008;33:7538–52.
[22] Guizz GL, Manno M, De Falco M. Intl J Hydrogen Energy 2009;34:3112–24.
[23] Doucet G, Etiévant C, Puyenchet C, Grigorie S, Millet P. Intl J Hydrogen Energy 2009;34:4983–9.
[24] Eroglu M, Dursun E, Sevencan S, Song J, Yazici S, Kilic O. Intl J Hydrogen Energy 2011;36:7985–92.